


Article

Two RSV Platforms for G, F, or G+F Proteins VLPs

Binh Ha ¹, Jie E. Yang ², Xuemin Chen ¹, Samadhan J. Jadhao ¹, Elizabeth R. Wright ^{2,3,4,*}  and Larry J. Anderson ^{1,*}

¹ Division of Pediatric Infectious Diseases, Emory University School of Medicine and Children's Healthcare of Atlanta, Atlanta, GA 30322, USA; binh.ha@emory.edu (B.H.); xchen26@emory.edu (X.C.); samadhan.jadhao@emory.edu (S.J.J.)

² Department of Biochemistry, University of Wisconsin, Madison, WI 53706, USA; jyang525@wisc.edu

³ Cryo-Electron Microscopy Research Center, Department of Biochemistry, University of Wisconsin, Madison, WI 53706, USA

⁴ Morgridge Institute for Research, Madison, WI 53715, USA

* Correspondence: erwright2@wisc.edu (E.R.W.); larry.anderson@emory.edu (L.J.A.);
Tel.: +1-608-265-0666 (E.R.W.); +1-404-712-6604 (L.J.A.);
Fax: +1-608-265-4693 (E.R.W.); +1-404-727-9223 (L.J.A.)

Received: 22 June 2020; Accepted: 17 August 2020; Published: 19 August 2020



Abstract: Respiratory syncytial virus (RSV) causes substantial lower respiratory tract disease in children and at-risk adults. Though there are no effective anti-viral drugs for acute disease or licensed vaccines for RSV, palivizumab prophylaxis is available for some high risk infants. To support anti-viral and vaccine development efforts, we developed an RSV virus-like particle (VLP) platform to explore the role RSV F and G protein interactions in disease pathogenesis. Since VLPs are immunogenic and a proven platform for licensed human vaccines, we also considered these VLPs as potential vaccine candidates. We developed two RSV VLP platforms, M+P and M+M2-1 that had F and G, F and a G peptide, or a truncated F and G on their surface. Immunoblots of sucrose gradient purified particles showed co-expression of M, G, and F with both VLP platforms. Electron microscopy imaging and immunogold labeling confirmed VLP-like structures with surface exposed projections consistent with F and G proteins. In mice, the VLPs induced both anti-F and -G protein antibodies and, on challenge, reduced lung viral titer and inflammation. These data show that these RSV VLP platforms provide a tool to study the structure of F and G and their interactions and flexible platforms to develop VLP vaccines in which all components contribute to RSV-specific immune responses.

Keywords: respiratory syncytial virus (RSV); virus-like particles (VLPs); vaccine; electron microscopy (EM); mouse model

1. Introduction

Respiratory Syncytial Virus (RSV) [1] was quickly recognized as a significant pediatric pathogen after its discovery in the 1950s. RSV causes upper and lower respiratory tract infections including bronchitis, bronchiolitis, and pneumonia. Most children are infected by two years of age [2] but then re-infections occur throughout life. The elderly and individuals with chronic cardiac or pulmonary disease, or immune-compromising conditions are at higher risk for severe complications with re-infection. It is estimated that globally, per year, there are more than 33 million cases of RSV-associated infections that result in 95,000–150,000 RSV deaths in children less-than five years of age, mostly in developing countries [3]. RSV-related deaths are rare in the United States. However, RSV infections are responsible for an estimated 60,000–170,000 hospitalizations each year in children less-than five years of age [4,5]. Additionally, infants hospitalized with RSV infection are prone to subsequent development of obstructive airway diseases and asthma [6,7]. The substantial global disease burden has made RSV

a high priority for vaccine and anti-viral drug development. Currently, there are no effective anti-viral drugs for the acute infection or vaccines available [8]. Palivizumab prophylaxis is available for some high risk infants.

Understanding the biology and pathogenesis of RSV infection is important to development of vaccines and anti-viral drugs. RSV is a single-stranded, negative sense RNA virus belonging to genus *Orthopneumovirus* in the family *Pneumoviridae* with two distinct antigenic groups, A and B [9]. The RSV genome of approximately 15.2 kb includes 10 genes that encode for 11 proteins [10]. Three glycoproteins, fusion (F), attachment (G), and small hydrophobic (SH), are expressed on the virion envelope. The F and G proteins, however, are the only ones shown to induce effective neutralizing antibodies and longer-term protective immunity. The F protein is more conserved among RSV strains and induces cross-protective immunity and is the most effective at inducing neutralizing antibodies. The SH protein does induce some protection likely through Fc receptor mediated activity, such as antibody-dependent cellular cytotoxicity or complement activation [11]. Most neutralizing antibodies in human serum specimens are against the pre-fusion form of F [12]. In fact, pre-fusion F is currently a prime candidate for RSV subunit vaccines [13]. The G protein, though eliciting less potent neutralizing antibodies, has been shown to be an important factor for RSV disease pathogenesis, making it also a candidate for inclusion in an RSV vaccine [14]. Structurally, the G protein consists of a conserved region that contains a CX3C chemokine motif that enables its binding to the CX3C chemokine receptor, CX3CR1, which induces responses similar to those induced by the CX3C chemokine fractalkine [15]. In fact, our studies in the BALB/c mouse model indicate that G induces disease causing inflammatory responses that can be blocked by inhibiting G binding to CX3CR1 with passive administration of an anti-G monoclonal antibody [16–18], G peptide vaccine-induced antibodies [19–21], or by mutating the CX3C motif. G binding to CX3CR1 also mediates infection of primary human airway epithelial cells and CX3CR1 is considered an RSV receptor in these cells [22,23]. The functions of F and G in infection and disease pathogenesis continue to be important areas for investigation but their interaction has received little attention. F and G interactions are suggested by co-immunoprecipitation experiments, cryo-electron tomography (cryo-ET) studies of G's effect on F in virions, and the need for both a mutated F and G to induce lung mucus in mice [16,24–27].

We chose to develop RSV platform based VLPs to support studies of F and G interactions and to develop candidate vaccines. An RSV platform VLP should mimic the natural structure of the F and G proteins better than other platforms and all components have the potential to contribute to vaccine-induced RSV immunity. RSV VLPs have been developed using the Newcastle disease, influenza, or bacteriophage P22 platforms and incorporated the RSV F and/or G proteins or M and M2 proteins [28–30]. RSV VLPs produced from an RSV platform have been described and were composed of F, M, nucleoprotein (N), and phosphoprotein (P) proteins; F, G, and M proteins; or F, M, and P proteins [31–33]. We describe successful development of RSV VLPs that incorporated F and/or G with the RSV M and P or M and M2-1. We developed VLPs with M and M2-1, in addition to those previously described with M and P, because M2-1 is thought to be important for structural stability of RSV [26]. We successfully generated RSV VLPs with surface expression of F and G, F and a G peptide, and F without most of its extracellular domain and G and demonstrated their immunogenicity and ability to protect RSV challenged mice.

2. Materials and Methods

2.1. Cells, Media, and Plasmids

All restriction enzymes were obtained from New England Biolabs (Ipswich, MA, USA). 293F cells were stably transfected with plasmid pcDNA6/TR and cultured in freestyle 293 media (Gibco, Thermo Fisher Scientific, Waltham, MA, USA) on a shaker at 37 °C, 8% CO₂. pcDNA3.1 DNA plasmids containing codon-optimized RSV genes M, M2-1, P, G, and F from the A2 strain were from Dr. Martin Moore (now at Meissa Vaccines Inc, Redwood City, CA, USA). The plasmids were digested by KpnI

and XhoI enzymes and cloned into KpnI and XhoI double digested pcDNA4/TO or pcDNA5/TO vector. Human codon-optimized truncated G consisting of amino acids 1-86+155-206 was synthesized by Genescript (Piscataway, NJ, USA). The gene provided in pUC57 plasmid was digested by BamHI and XhoI restriction enzymes and cloned into BamHI and XhoI digested pcDNA5/TO vector. All genes were sequence confirmed prior to transfection. To generate VLPs, 293F cells were sequentially and stably transfected with the RSV genes noted below. We chose stably instead of transiently transfected cells because they provide a more consistent source of VLPs with a known composition.

2.2. Virus-Like Particle Expression and Purification

A total of $20\text{--}30 \times 10^6$ 293F cells were induced with 2 $\mu\text{g}/\text{mL}$ of doxycycline for 72 h. Cells were centrifuged at $300\times g$ for 10 min and the VLP-containing media was filtered through 0.45 μm filter followed by centrifugation through 20% sucrose cushion at $12,200\times g$ for 2 h at 4 °C (SW Ti 32 rotor, Optima L-90K Ultracentrifuge, Beckman Coulter, (Indianapolis, IN, USA)). The top layer of cell media and sucrose was thoroughly removed and the pellet was soaked in sterile PBS for 1 h on ice and resuspended. For sucrose gradient experiments, preparation of a linear sucrose gradient was described previously [34], 1 mL of the gradient was removed before the resuspended VLPs were layered onto the gradient and centrifuged with a Beckman Coulter SW 41 rotor at $11,000\times g$ for 12 h at 4 °C. A total of 10 1-mL fractions were removed from top, diluted 3 \times with sterile PBS, and centrifuged at $12,000\times g$ for 1 h at 4 °C on a bench-top centrifuge. Supernatants were completely removed and pellets were soaked in sterile PBS for 1 h on ice before being resuspended.

2.3. Antibodies and Immunoblotting

The anti-G protein monoclonal antibody (mAb) 3D3 was provided by Trellis Bioscience (Redwood City, CA, USA); the anti-F protein mAb motavizumab was provided by MedImmune (Gaithersburg, MD, USA); palivizumab was from Dr. Martin Moore's laboratory; rabbit serum anti-M antibody was provided by Dr. Oomens (Oklahoma State University); and goat anti-RSV antibody was obtained from Millipore (Burlington, MA, USA). All anti-species fluorescence-conjugated secondary antibodies used in immunoblotting were obtained from LI-COR biosciences (Lincoln, NE, USA). All HRP-conjugated secondary antibodies used in enzyme-linked immunosorbent assays (EIAs) were obtained from Jackson ImmunoResearch (West Grove, PA, USA). For immunoblotting experiments, VLP samples were mixed with 2 \times Laemmli sample buffer (Bio-Rad, Hercules, CA, USA) and boiled at 95 °C for 5 min. Samples were run on SDS-PAGE, transferred to a nitrocellulose membrane, blocked for 30 min in blocking buffer (5% dry milk in TTBS, 0.1% Tween-20 in tris-buffered saline). The primary antibody was added and incubated for overnight at 4 °C, membrane was washed 3 \times in TTBS, secondary antibody added and incubated for 30 min, and the membrane washed 3 times in TTBS. Signals were visualized by Odyssey CLX imaging system (LI-COR).

2.4. F, Ga, and Gb Antibody EIAs

The secreted form of F, Ga, or Gb protein antigens was produced from stably-transfected 293F cells in serum-free media and coated onto a 96-well microtiter plate in coating buffer (15 mM Na_2CO_3 , 35 mM NaHCO_3 , 3 mM NaN_3 , pH 9.4–9.6). The plates were incubated in 2% nonfat dry milk dissolved in PBS blocking solution for 2 h at 37 °C, washed with PBS-T (PBS + 0.15% Tween-20), and serum specimens at 1:200 dilution added to the wells, incubated for 1 h at 37 °C, the plates washed with PBS-T, and goat anti mouse IgG-HRP (1:5000) added and incubated for 1 h at 37 °C. Color was developed with *o*-Phenylenediamine dihydrochloride (OPD) (Sigma-Aldrich, St. Louis, MO, USA) substrate and the reaction stopped after 30 min at RT with 4N H_2SO_4 . The absorbance was measured at an optical density (OD) of 490 nm and the geometric mean of the OD_{490} was calculated from the triplicate wells.

2.5. RSV Neutralizing Antibody Assay

Heat inactivated sera were serially two-fold diluted starting with a 1:10 dilution in minimum essential media (MEM) (Gibco, Thermo Fisher Scientific, Waltham, MA, USA) containing 0.5% fetal bovine serum (FBS) (R&D Systems, Minneapolis, MN, USA), incubated with RSV/A2 (100 TCID₅₀) for 1 h at RT, and inoculated in triplicates onto non-confluent HEp-2 monolayers in 96-well plates for 1 h at 37 °C in a 5% CO₂ incubator. MEM containing 5% FBS was added to all the wells and cells were incubated for 3 days at 37 °C in a 5% CO₂ incubator. The plate was washed with PBS and fixed with 4% paraformaldehyde. The plate was washed with PBS and incubated in PBS containing 0.3 M glycine for 30 min at RT followed by incubation in blocking solution (1% gelatin + 1% casein + 1% dry milk in PBS) for overnight at 4 °C. The plate was then incubated with goat anti RSV antibody (1:5000) followed with donkey anti-goat IgG-HRP secondary antibody (1:5000). Both primary and secondary antibodies were diluted in blocking buffer supplemented with 0.15% Tween-20. Color was developed with OPD substrate and neutralization defined as a ≥ 50% reduction in OD value. The titer was estimated using the Reed and Muench method [35]. The geometric means ± SEM for all animals in a group at any given time were calculated.

2.6. VLP Negative-Stain Transmission Electron Microscopy

Conventional negative-stain transmission electron microscopy (TEM) and immunolabeling was performed, as described previously [36]. Briefly, 4 µL of diluted samples was applied onto glow-discharged EM grids (FCF300-Cu; Electron Microscopy Sciences, Hatfield, PA, USA), washed with distilled pure water, stained in droplets of 0.75% uranyl formate (UF, pH 4~5) or 1% phosphotungstic acid (PTA, pH 6~7) for 1-min. The staining was carried out on an ice block. The grids were then blotted from the backside and air-dried inside a petri dish for at least 30-min at room temperature to minimize the negative-stain artifacts of flattening and stacking [37]. The negative-stain grids were imaged in low-dose mode (50 e⁻/Å), using a FEI Tecnai 12 transmission electron microscope (Thermo Fisher Scientific, previously FEI, Hillsboro, OR, USA) at 120 kV, images were acquired on a 4k × 4k Gatan OneView Camera (Pleasanton, CA, USA).

2.7. Immunogold Labeling Transmission Electron Microscopy

VLPs were subjected to immunogold labeling. The procedures were adapted from a previous published method [38]. A total of 4 µL of diluted samples was incubated on glow-discharged EM grids (FCF300-Ni; Electron Microscopy Sciences, Hatfield, PA, USA) for 5 min at room temperature. The grids were incubated on droplets of 20 mM glycine for 10-min, followed by a 30-min blocking in 5% bovine serum albumin in PBS without calcium chloride, without magnesium chloride (DPBS, [-] Ca, [-] Mg). The grids were floated onto 30 µL droplets of palivizumab (1:50) or Motavizumab (40 µg/mL) in 5% BSA in DPBS ([-] Ca, [-] Mg) overnight at 4 °C. After three washes with 1% BSA in DPBS ([-] Ca, [-] Mg), 5-min per wash, the grids were placed on 30 µL of droplets of 6-nm gold beads conjugated with goat anti-human polyclonal IgG antibody (Electron Microscopy Sciences, Hatfield, PA) at 1:100 dilution in 5% BSA in DPBS ([-] Ca, [-] Mg), for 1-h at room temperature. Then the grids were washed three times with 1% BSA in DPBS ([-] Ca, [-] Mg), and stained with 1% PTA (pH 6~7), as described above. The negative-stain grids were imaged in low-dose mode (50 e⁻/Å), using a FEI Tecnai 12 transmission electron microscope (Thermo Fisher Scientific, previously FEI, Hillsboro, OR) at 120 kV, images were acquired on a 4k × 4k Gatan OneView Camera (Pleasanton, CA, USA).

2.8. VLP Morphology Characterization

Only purified particles with a clear presence of surface glycoproteins were quantified, measured, and analyzed. Particle 2D-projection surface area was measured in IMOD using the *imodinfo* command by making close-contour objects [39]. The circular equivalent diameter χ_A , defined as the diameter of a circle with the same area as the particle, was calculated per equation $\chi_A = \sqrt{\frac{4A}{\pi}}$, where A is the

surface area of the VLPs, expressed in units of nm [40]. Similarly, the maximum Feret's diameter, defined as the furthest distance between any two parallel tangents on the particle, was measured in IMOD, expressed in units of nm [40]. The distribution of the particle measurements was displayed in a histogram graph generated in Prism software (GraphPad Software, San Diego, CA, USA).

2.9. Virus

A recombinant virus of the RSV A2 backbone expressing the F protein from L19 virus (r19F) [41] was chosen as the challenge virus since it induces airway disease that parallels RSV infection in humans but is not seen with RSV A2. Stock virus was prepared by inoculating sub-confluent cultured HEp-2 cells with the recombinant RSV A2 at a multiplicity of infection (MOI) of 0.01 for 2 h at 37 °C in 5% CO₂ incubator using 0.5% FBS-containing MEM. 5% FBS MEM was added and cells were incubated at 37 °C with 5% CO₂ for three days. Cells were frozen and thawed twice at −80 °C and 4 °C, respectively, and centrifuged at 2000 rpm for 15 min at 4 °C to remove cellular debris. The supernatant was layered onto 20% sucrose and centrifuged at 12,200× *g* for 2 h at 4 °C. The pellet was resuspended in serum free MEM, divided into aliquots, and snap frozen in liquid nitrogen. The aliquots were stored at −80 °C until used. The infectivity titer of the inoculum was determined by serial 10-fold dilutions in sub-confluent HEp-2 cell cultures for three days and virus replication detected by EIA for RSV antigens with goat-anti RSV antibody. Titer was estimated from wells with absorbance > 3 standard deviations above the mean absorbance for wells without virus by the Reed and Muench method.

2.10. Animal Study

Four- to six-week old female BALB/c mice were purchased from Charles River Lab (Wilmington, MA, USA) and housed at Emory's Department of Pediatrics animal facility under food ad libitum in micro-isolator cages with auto sterilized water. All animal handling and procedures were carried out according to protocols approved by Emory University (Atlanta, GA, USA) Institutional Animals Care and Use Committee (IACUC), (PROTO201700401, approved on 06/12/2018). For challenge studies, mice were intranasally infected with 10⁶ TCID₅₀ RSV r19F A2, 40 µL in volume.

2.11. Real-Time PCR

Total RNA was extracted and purified from lung homogenates using Qiagen RNeasy kit (Qiagen, Hilden, Germany). RNA was reverse transcribed into cDNA using iScript™ cDNA synthesis kit (Bio-Rad) following the manufacturer's instruction. Quantitative PCR was carried out on a 7500 Fast Real-time PCR system (Applied Biosystems, Foster City, CA, USA) using Power SYBR Green PCR master mix (Applied Biosystems). C_T values were normalized using control β-actin C_T values from the same samples. RSV matrix M gene primers and amplification cycles were described previously [42]. Other primer pairs used were: β-actin, forward 5'-CAC CAA CTG GGA CGA CAT-3', reverse 5'-ACA GCC TGG ATA GCA ACG-3'. mRNA levels were expressed as the geometric mean ± SEM for all animals within a group.

2.12. Pulmonary Histopathology

Lungs were isolated and fixed in 10% neutral buffered formalin for 24 h. The lungs were then embedded in paraffin, sectioned, and stained with Periodic acid-Schiff (PAS). The slides were scanned on Hamamatsu Nanozoomer (Hamamatsu Corporation, Bridgewater, NJ, USA), analyzed by Aperio ImageScope software version 12.4.0.5043 (Leica Systems Inc., Buffalo Grove, IL, USA), and scored blinded to treatment on a 0–4 scale. They were subsequently converted to a 0–100% histopathology scale.

2.13. Statistical Analysis

Unless otherwise indicated, different groups were compared by Wilcoxon rank sum test or Wilcoxon matched pairs test. A *p*-value of <0.05 was considered statistically significant. Data are shown as means and standard errors of the mean (SEM).

3. Results

3.1. Generation of G and F Virus-Like Particles (VLPs) on RSV M and P or M and M2-1 Platforms

RSV VLPs were generated by sequentially transfecting 293F cells with codon-optimized DNA plasmids containing RSV genes. The order of transfection is listed in Table 1. Western blot studies suggested that we successfully developed VLPs with RSV M plus P or M plus M2-1 protein platforms with F or F and G (Figure 1A) but only to very low levels with G alone, a condition not observed with F in VLPs expressing only F (Figure 1C), i.e., detection of F or F and G in the supernatant and not the cell pellet of the induced 293F cells. VLPs are released from cells. Additionally, F or F and G were detected by Western blot in the pellet after centrifugation through a sucrose cushion indicating the proteins were incorporated into particles and not in solution in the media. Finally, F and M, or F, G, and M were detected by Western blot in the same fractions after sucrose gradient purification indicating presence of M in VLPs containing F and F and G (Figure 1A).

Table 1. Generation of VLPs. 293F/6TR cells were sequentially and permanently transfected with plasmid DNA coding for RSV proteins as shown in table. G_P: G protein peptide (aa 1-86+155-206).

| VLPs | Order of Transfection | | | |
|----------------------|-----------------------|-----|------|----------------|
| | 1st | 2nd | 3rd | 4th |
| M | M | | | |
| MFP | M | F | P | |
| MFPG | M | F | P | G |
| MFPG _P | M | F | P | G _P |
| MFM2-1 | M | F | M2-1 | |
| MFM2-1G | M | F | M2-1 | G |
| MFM2-1G _P | M | F | M2-1 | G _P |

Given the importance of G's central conserved domain in disease pathogenesis, we chose to develop a VLP that would focus the G immune response to this region. To this end, co-expressed F and G peptides with the intracellular, transmembrane, and first 20 amino acids of the extracellular domains (amino acids 1–86) plus amino acids 155–206 representing the central conserved domain (G_P). We successfully generated these VLPs with either the M+P or M+M2-1 platform as indicated by Western blot studies of sucrose gradient purified VLPs (Figure 1B).

The fact that G alone was inefficiently but with F was efficiently incorporated into the VLPs suggested that F facilitated generation of G VLPs. The importance of F in RSV VLP formation has been noted in an earlier study showing that the carboxyl terminal portion of F is required for VLP formation [31]. We hypothesized that the intracellular and transmembrane F would be sufficient to form G VLPs and generated a truncated F with its carboxyl terminus + transmembrane + first 26 amino acids of the extracellular domain (F_t) to co-express with full-length G. Our data with the M + P VLP platform show that with F_t, G is abundantly expressed in the VLPs (Figure 1C).

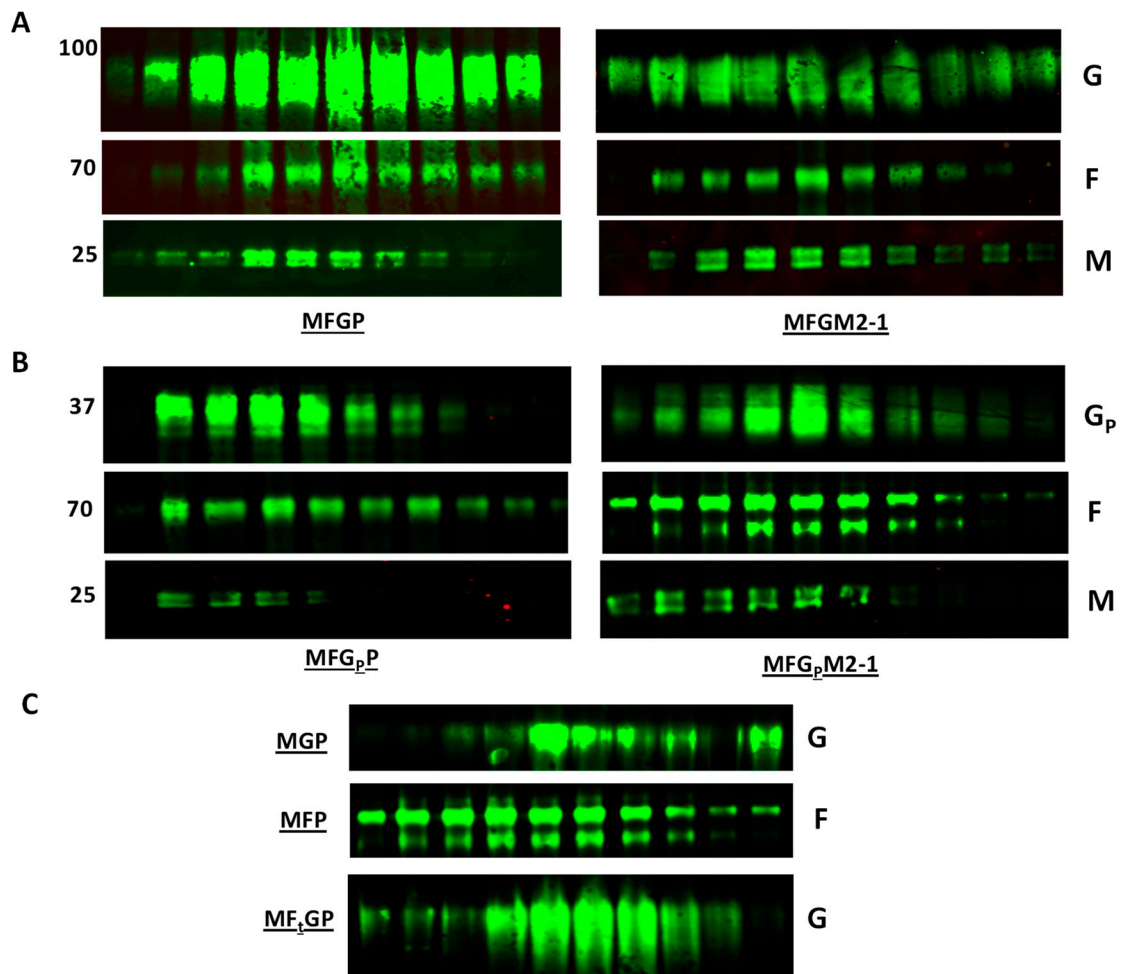


Figure 1. Generation and expression of F and G on RSV VLPs. 293F cell line expressing RSV gene M, F (or F_t), G (or G_p), and P or M2-1 were induced for 72 h in 2 µg/mL doxycycline. Cells were harvested and low-speed centrifugation performed to separate cells and VLPs-containing supernatant. VLPs were filtered through 0.45 µm filter to clear cell debris, layered on top of a 20% sucrose cushion and subjected to centrifugation at 12,200× *g* for 2 h, 4 °C. VLP pellets were resuspended in sterile PBS and subjected to centrifugation through a 20–60% sucrose gradient at 11,000× *g* for 12 h, 4 °C. A total of 10 fractions were collected and analyzed by immunoblotting using 3D3 (human anti-G antibody), motavizumab (human anti-F antibody), and rabbit serum anti-M antibody. (A) VLPs MFGP and MFGM2-1. Note that high levels G, F, and M are detected in similar fractions, (B) VLPs MFG_pP and MFG_pM2-1. G_p, truncated G: aa 1-86+155-206. Note that high levels G, F, and M are detected in similar fractions, (C) MGP, MFP, and MF_tGP VLPs. F_t, truncated F: aa 496–574. Note that the expression level of G is less without F (MGP) than when F_t is co-expressed with G (MF_tGP).

3.2. Electron Microscopy Characteristics of G and F on VLPs

To confirm generation of F and G VLPs, negative-stain transmission electron microscopy (NS-TEM) was performed on both MFGP and MFGM2-1 particles. NS-TEM examination showed that the VLPs with both constructs have the expected protein-like electron densities corresponding to surface glycoprotein F and G on their surface (Figure 2A,B,E,F). We confirmed the presence of the two surface glycoproteins on the VLP surface with immunogold labeling as illustrated in Figure 2.

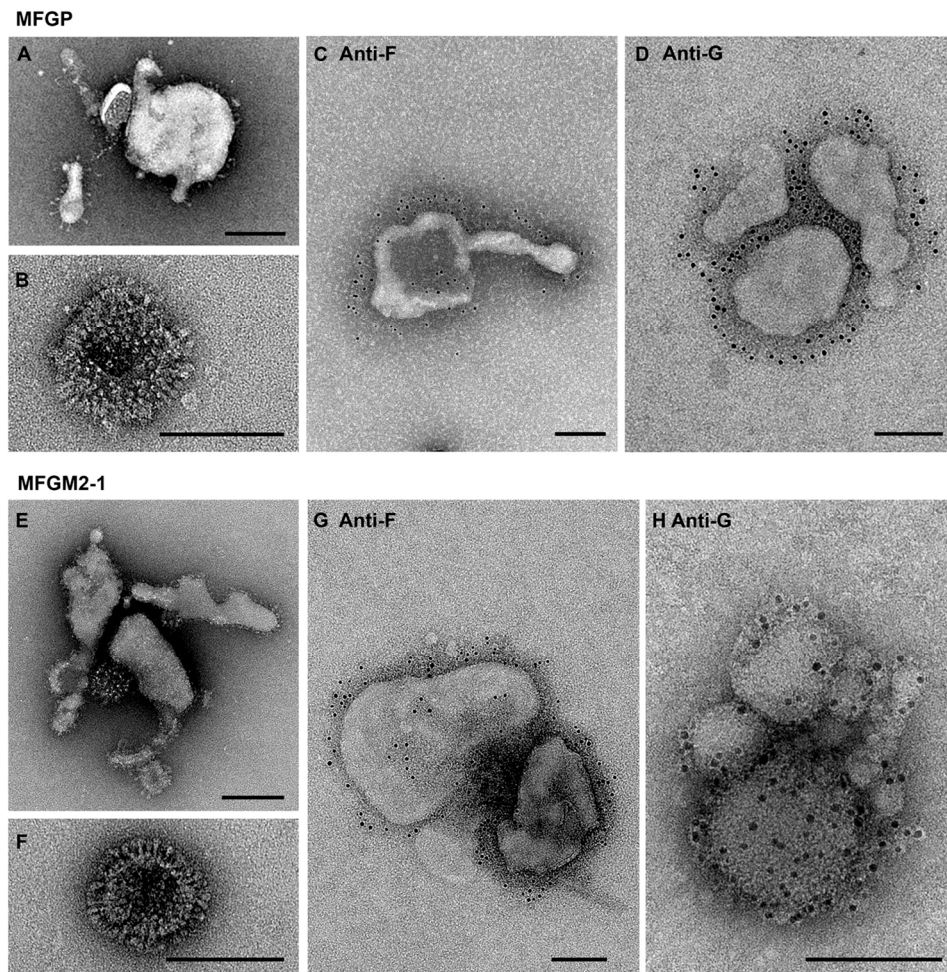


Figure 2. Electron microscopy studies show glycoproteins on the surface of RSV VLPs. Negative stain electron microscopy images showed that both MFGP and MFGM2-1 VLPs were of various shapes and sizes, displaying clear spikey glycoprotein densities on the surface (A,B,E,F). Immunogold labeling confirmed the presence of glycoprotein F with Palivizumab (C,G), and glycoprotein G with 3D3 (D,H) on the surface of MFGP and MFGM2-1, respectively. All scale bars are 100 nm.

To quantify size and morphologic characteristics, purified VLPs were imaged using 2D NS-TEM (Figure 3). VLP surface area and maximum Feret's diameter (MFD) showed large variation in size for MFGP VLPs, with circular equivalent diameter (CED) ranging from 32 to 298 nm (Figure 3A). CED is defined as the diameter of a circle with the same area as the particle. Approximately, 80% of MFGP VLPs ($n = 295$) are 50~200 nm in CED and 100~500 nm in MFD, with a median of 91.6 nm and 300.8 nm, respectively (Figure 3). The other VLP platform MFGM2-1 showed a similar variation in size and shape, with CED from 28 to 263 nm and MFD from 88 to 836 nm (Figure 3). Almost 90% of MFGM2-1 ($n = 151$) fell in the range of 32–160 nm in CED (the median = 83.05 nm) and 88–490 nm in MFD (the median = 263.4 nm). Despite the artifacts introduced by 2D NS-TEM such as stacking and flattening, it is clear that MFGP and MFGM2-1 VLPs are highly variable in shape and size.

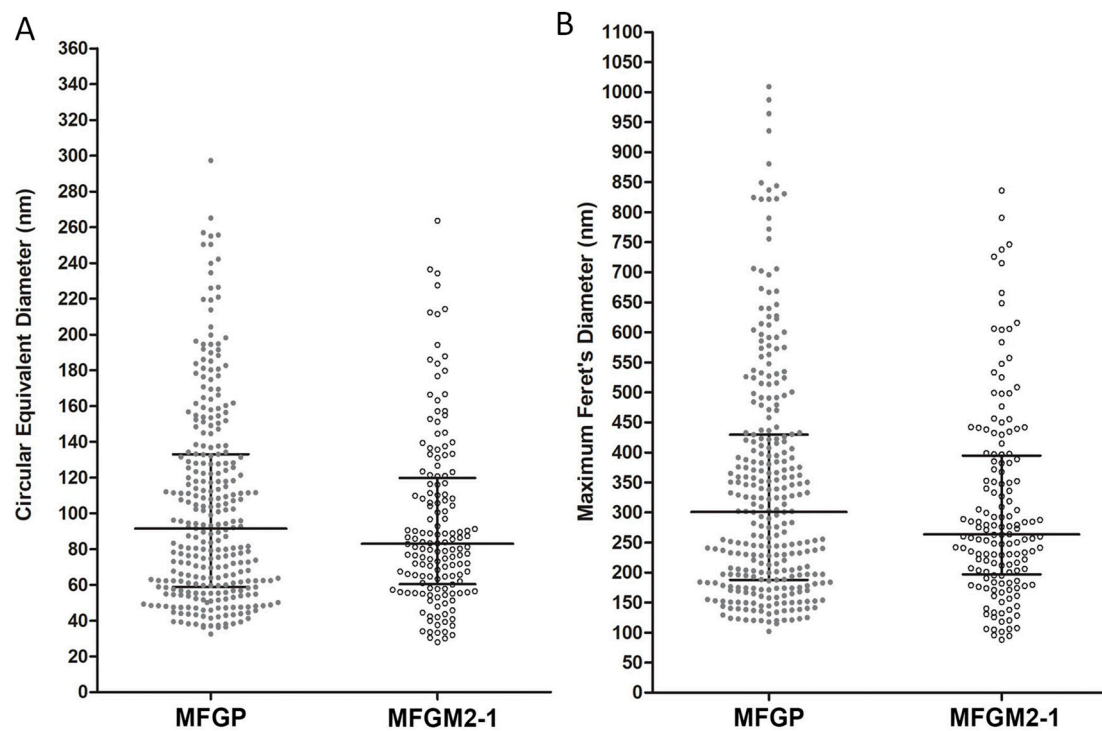


Figure 3. Size distribution of MFGP and MFGM2-1 VLPs. Morphological analysis was performed on MFGP and MFGM2-1. Circular equivalent diameter (A) and maximum Feret's diameter (B) were measured and analyzed from negative stain electron microscopy images of MFGP ($n = 295$) and MFGM2-1 ($n = 151$). Median and interquartile ranges are shown in the graph. The median of the circular equivalent diameter is 91.6 nm for MFGP, and 83.05 nm for MFGM2-1. The median of the maximum Feret's diameter is 300.8 nm for MFGP, and 263.4 nm for MFGM2-1.

3.3. VLPs Are Immunogenic

To determine the immunogenicity of the VLPs, we immunized BALB/c mice ($n = 4$) with the VLPs as detailed in Table 2. All immunized animals were challenged with 10^6 TCID₅₀ of RSV r19F at four weeks after the second, booster, immunization (Figure 4A). Blood specimens were collected before challenge and tested for F, a group A G (Ga), and a group B G (Gb) protein binding antibodies by EIA and neutralizing antibodies by a micro-neutralization assay. All immunized animals except for those immunized by control M VLPs developed antibodies against F and Ga. Only one animal produced antibodies against Gb antigen (Figure 4B). Additionally, the short G peptide (G_P) seemed to be more efficient at inducing anti-Ga antibody than its full-length counterpart ($p > 0.05$), indicating that the central conserved domain of G is an effective immunogen. Furthermore, VLP antigens that contained P seemed to induce antibodies against F better than those that contained M2-1 but this difference was not significant (Figure 4B). In this study, the VLPs induced low levels of neutralizing antibodies. As shown, sera from animals in groups immunized with MFP and MFM2-1G_P did not possess neutralizing activity but sera from other groups had one or two animals with some low titer neutralizing activity (Figure 4C). This difference was not significant.

Table 2. Immunization schedule. Mice were divided into seven groups and immunized as shown above and in Figure 4A. Other groups: MFP, MFGP, MFG_PP, MFM2-1, MFGM2-1, or MFG_PM2-1. IM, intramuscular.

| Group | <i>n</i> | Dose (Per Mouse) | Immunization Days | Route | RSV Challenge TCID ₅₀ /Mouse | Days of Harvest |
|--------|----------|------------------|-------------------|-------|---|-----------------|
| M | 4 | 50 µg VLPs | 0, 21 | IM | 10 ⁶ at day 49 | 54 |
| Others | " | " | " | " | " | " |

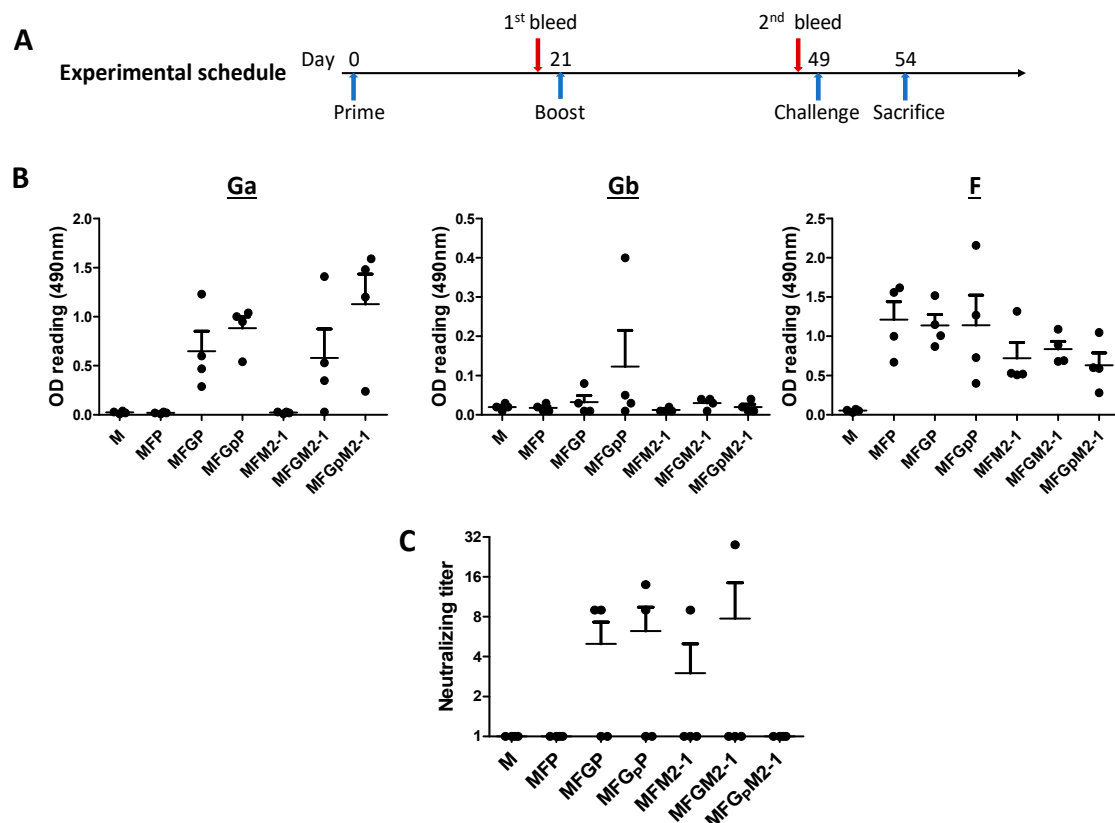


Figure 4. VLP-immunized mice generate serum antibodies against G and/or F. (A) Schematic schedule of animal experiments. (B) Sera from immunized animals (diluted 1:200) were tested by ELISA for Ga, Gb, or F protein-binding antibodies. After blocking, plates were incubated with goat anti mouse IgG-HRP secondary antibody. OPD substrate was used to develop reaction and absorbance at 490 nm was read. Note the VLPs efficiently induced antibodies against Ga and F but not Gb. (C) Sera from immunized animals were heat inactivated at 56 °C for 30 min followed by two-fold serial dilution in triplicate. The dilutions were incubated with 100 TCID₅₀ of RSV A2 virus for 1 h at RT. The mixtures were then transferred to monolayer HEp-2 cell and incubated for 1 h at 37 °C in 5% CO₂. 5% FBS + MEM media was added to the cells followed by incubation for 72 h at 37 °C in 5% CO₂. Cells were fixed and ELISA was performed using goat anti-RSV antibody and HPR-conjugated donkey anti-goat secondary antibody. Reaction was developed by OPD and absorbance read at 490 nm. Neutralizing titers were calculated using Reed–Muench method. Note low levels of neutralizing antibodies were induced by the VLPs.

3.4. VLP Immunization Reduces Lung Viral Titers

Next, we investigated the ability of the VLPs to prevent virus replication after challenge. We purified total RNA from lung homogenates and performed RT-PCR using RSV M matrix protein primers and β -actin as control. Figure 5 shows that the relative cycle threshold (C_T) values were significantly higher indicating less virus replication in animal groups that had P protein as part of the

antigen VLPs, i.e., MFP, MFGP, and MFG_PP compared to the control antigen (M only VLPs). A higher value of C_T correlates with low copy of the gene being evaluated. Additionally, there were significant differences between MFG_PP and MFP or MFGP (Figure 5), indicating that anti-G antibodies participate in viral clearance in the lungs and that G_P was more effective in facilitating virus clearance than full length G. Moreover, VLP antigens that contained M2-1 protein, i.e., MFM2-1, MFGM2-1, and MFG_PM2-1 had C_T values similar to those from the comparable construct on the M+P platform, but not significantly higher than control C_T values (Figure 5).

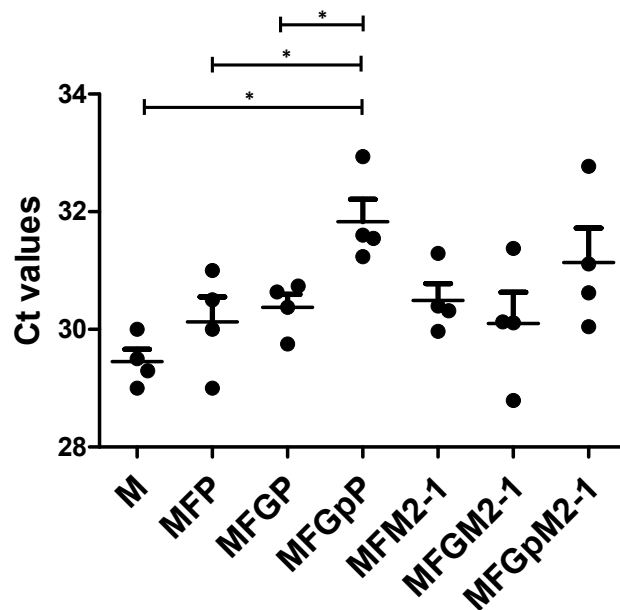


Figure 5. Immunized animals have significantly less lung viral titer. Lungs from immunized animals were homogenized as described in materials and methods. Aliquots stored at -80°C were thawed and total RNA was extracted from lung. RNAs were then reverse transcribed into cDNAs. These were used as templates in RT-PCR using CYBR green and a pair of RSV matrix protein M specific primers as described. In parallel, similar reactions were performed using a pair of β -actin specific primers as controls. Results were expressed as relative amount of RSV M compared to β -actin. * $p < 0.05$. Note the VLPs with G_P appeared most effective at reducing virus replication as indicated by PCR C_T values.

3.5. VLP Immunization Reduces Lung Inflammation

One of the manifestations of RSV infection with r19F virus is the overproduction of mucin [41], therefore, we examined pulmonary inflammation in challenged animals by Periodic acid-Schiff staining (PAS). The stained slides were analyzed by Aperio ImageScope software (Leica, Germany) and scored blindly using 0–4 severity scale and then converted to 0–100 histopathology scale. Here, positive PAS staining was observed in the lungs of all animals, indicating the presence of mucin. However, animals immunized with VLPs expressing F and/or G showed decreased staining compared to animals immunized with the control VLPs expressing only M. (Figure 6A,B). Only MFG_PP- and MFG_PM2-1-immunized animals had a significant reduction in PAS staining when compared to control animals (Figure 6A,B). These data show that F plus G_P VLPs were the most effective at reducing both lung virus replication and mucin production.

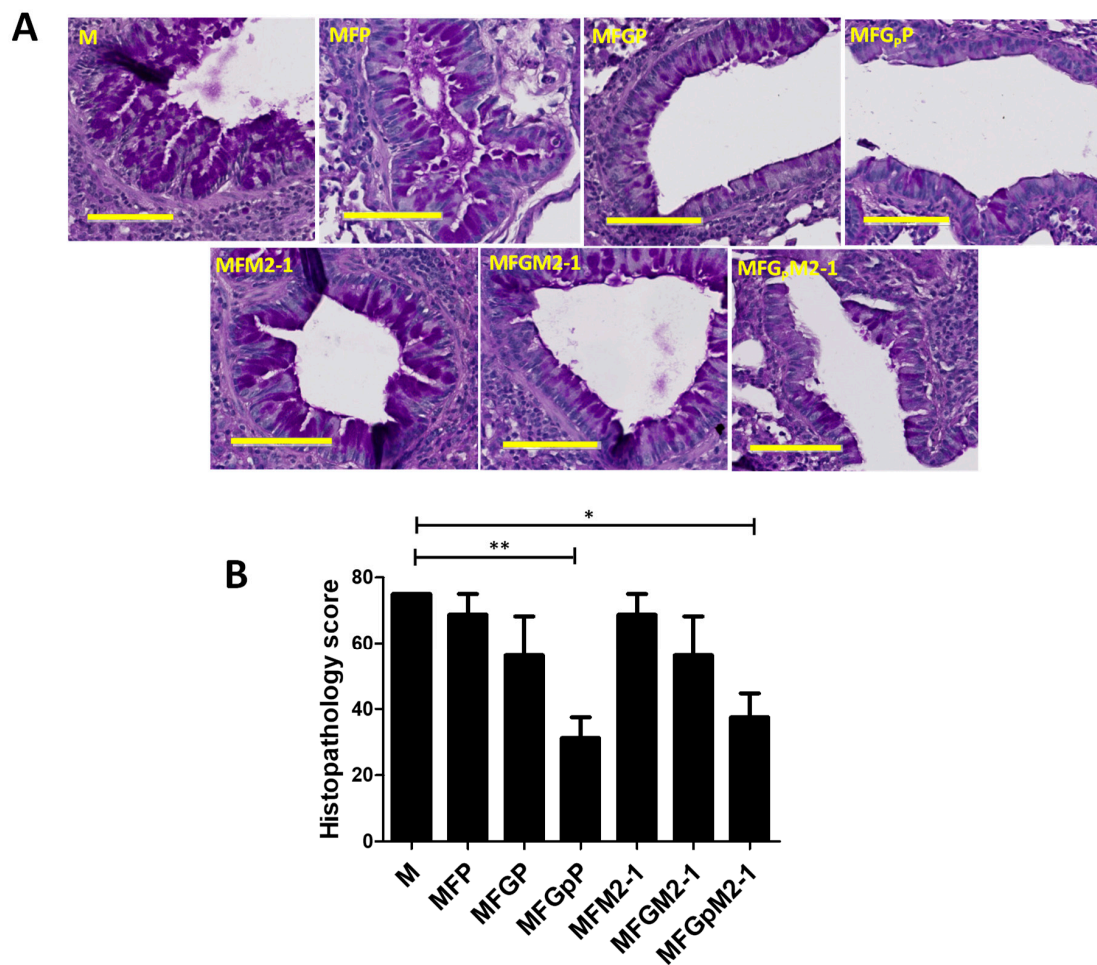


Figure 6. Immunized animals show a significant reduction in lung inflammation. Female BALB/c mice (4–6 weeks) were divided in 7 groups ($n = 4$), immunized, and challenged as summarized in Table 2. Lungs were collected, fixed, and stained with periodic-acid Schiff (PAS) staining as described in the materials and methods. The slides were analyzed by Aperio ImageScope software and scored blindly on a 0–4 scale and subsequently converted to a 0–100% histopathology, Bar = 100 μ m scale. (A) Representative images from corresponding groups. (B) Quantitative data converted from histopathology scale. * $p < 0.05$, ** $p < 0.01$. Note the VLPs with Gp appeared most effective at reducing lung mucin levels.

4. Discussion

We developed two RSV-based VLP platforms M+P and M+M2-1 expressing F and G, F and G peptide, or Ft and G. The EM studies show surface projects and variability in size and shape. The virus is also pleomorphic in size and shape [43]. Important to structural studies and vaccine development, these two platforms support the generation of VLPs with different F and G constructs. For structural studies, generation of G and truncated F (F_t) VLPs makes it possible to study G without most of the F ectodomain. These VLPs provide a tool to study structure, function, and immunogenicity of G with minimal influence from extracellular F. Studies of G with Ft also provide the framework to identify changes associated with the addition of F. From a vaccine perspective, we wanted to be able to focus immune responses to certain regions of G. Given the importance of the central conserved domain of G to disease pathogenesis [17,22,23,42,44], we chose to focus an immune response to this region. We successfully generated VLPs with a truncated G that expressed a peptide from the central conserved domain of G on its surface and immunization with this VLP compared with one with full-length G reduced lung virus titer and lung inflammation more effectively, though not significantly.

This improved protection is not surprising since VLPs with Gp induced higher titer of anti-G antibodies which should be against central conserved domain of G. Antibodies to this region of G have been shown to both decrease virus replication and lung inflammation in mice [16,17,19,21].

The RSV M+P VLP platform was described earlier [31] but the RSV M+M2-1 VLP platform was not. The M2-1 protein has transcription anti-termination activity and directly interacts with M, providing a link to the RNA-containing nucleocapsid [26,43,45–47]. The M2-1 protein's interaction with M provides a basis for considering ways it might support M+M2-1 VLP formation, e.g., by stabilizing M on the VLP surface. How P facilitates VLP formation has not been determined. P does have a crucial role in RSV polymerase activity by interacting with both nucleocapsid (N) and polymerase (L) proteins [48–50] and also cooperates with M2-1 [51]. However, these roles do not suggest how it might support VLP formation when co-expressed with M.

Negative stain EM studies revealed that the two VLP platforms expressed the surface glycoproteins F and G equally well with no structural differences observed. Similarly, our mouse studies show that both VLPs were immunogenic and induced serum antibodies against both F and G proteins to similar levels and were effective in decreasing lung virus and inflammation in RSV challenged mice. Interestingly, the VLPs with Gp compared to VLPs with full length G induced higher antibody titers and were more effective in decreasing lung virus and lung inflammation. The M2-1 protein's ability to induce short term protective T cell immunity in mice [30,52,53] might theoretically be advantageous in a vaccine. Whether this is an advantage for M+M2-1 versus M+P VLPs requires further study. We did not measure T cell responses in this study. Of note, the G protein sequences used here are from a group A strain (A2) and these G sequences efficiently induced antibodies against a group A but not a group B G protein. This suggests that G used in an RSV vaccine will likely need to have both group A and B sequences. Much of CCD-G is conserved within but not between groups. We also tested serum neutralizing antibody titers and observed that immunized animals developed low levels of neutralizing antibodies. VLPs with a pre-fusion stabilized F protein might be more effective at inducing neutralizing antibodies [54–56]. Further study is needed to determine the differences between the two platforms that may affect structure, function, immunogenicity, or other features of the VLPs, and to improve immunogenicity of the VLPs for a vaccine.

In summary, we successfully developed VLPs expressing F and/or G with two RSV platforms, co-expression of the M+P proteins or M+M2-1 proteins. With both platforms we were able to modify F and/or G to focus specific structural and antigenic features of the proteins. These platforms provide a flexible way to study the structure and function of these two proteins and to develop RSV subunit vaccines.

Author Contributions: B.H., J.E.Y., E.R.W., and L.J.A. participated in conceptualization, validation, formal analysis, investigation, data curation; B.H., E.R.W., and L.J.A. participated in project administration; B.H. wrote the initial draft; B.H., L.J.A., J.E.Y., and E.R.W. participated in data analysis and interpretation. B.H., J.E.Y., X.C., S.J.J., E.R.W., and L.J.A. participated in the methodology, review, and editing; L.J.A. and E.R.W. participated in funding acquisition. All authors have read and agreed to the published version of the manuscript.

Funding: This work was supported in part by Emory University and Children's Healthcare of Atlanta. L.J.A. receives support from NIH U19 AI 095227 and through the Vaccine and Treatment Evaluation Units (VTEU) award to Emory University (HHSN272201300018I). This work was also supported by the University of Wisconsin, Madison and public health service grant R01 GM114561 to E.R.W. from the NIH.

Acknowledgments: The authors gratefully acknowledge use of facilities and instrumentation at the UW-Madison Wisconsin Centers for Nanoscale Technology (wcnt.wisc.edu), which is partially supported by the NSF through the University of Wisconsin Materials Research Science and Engineering Center (DMR-1720415). We would also like to thank the Pathology core lab at Emory University for histological services and support.

Conflicts of Interest: The authors declare no conflict of interest. The funders had no role in the design of the study; in the collection, analyses, or interpretation of data; in the writing of the manuscript, or in the decision to publish the results.

References

1. Torsvik, V.; Ovreas, L.; Thingstad, T.F. Prokaryotic diversity—Magnitude, dynamics, and controlling factors. *Science* **2002**, *296*, 1064–1066. [[CrossRef](#)]
2. Hall, C.B.; Simoes, E.A.; Anderson, L.J. Clinical and epidemiologic features of respiratory syncytial virus. *Curr. Top. Microbiol. Immunol.* **2013**, *372*, 39–57. [[CrossRef](#)] [[PubMed](#)]
3. Shi, T.; McAllister, D.A.; O'Brien, K.L.; Simoes, E.A.F.; Madhi, S.A.; Gessner, B.D.; Polack, F.P.; Balsells, E.; Acacio, S.; Aguayo, C.; et al. Global, regional, and national disease burden estimates of acute lower respiratory infections due to respiratory syncytial virus in young children in 2015: A systematic review and modelling study. *Lancet* **2017**, *390*, 946–958. [[CrossRef](#)]
4. Stockman, L.J.; Curns, A.T.; Anderson, L.J.; Fischer-Langley, G. Respiratory Syncytial Virus-associated Hospitalizations Among Infants and Young Children in the United States, 1997–2006. *Pediatr. Infect. Dis. J.* **2012**, *31*, 5–9. [[CrossRef](#)] [[PubMed](#)]
5. Hall, C.B.; Weinberg, G.A.; Iwane, M.K.; Blumkin, A.K.; Edwards, K.M.; Staat, M.A.; Auinger, P.; Griffin, M.R.; Poehling, K.A.; Erdman, D.; et al. The burden of respiratory syncytial virus infection in young children. *N. Engl. J. Med.* **2009**, *360*, 588–598. [[CrossRef](#)] [[PubMed](#)]
6. Jarthi, T.; Gern, J.E. Role of viral infections in the development and exacerbation of asthma in children. *J. Allergy Clin. Immunol.* **2017**, *140*, 895–906. [[CrossRef](#)] [[PubMed](#)]
7. Wu, P.; Hartert, T.V. Evidence for a causal relationship between respiratory syncytial virus infection and asthma. *Expert Rev. Anti Infect. Ther.* **2011**, *9*, 731–745. [[CrossRef](#)]
8. Mazur, N.I.; Higgins, D.; Nunes, M.C.; Melero, J.A.; Langedijk, A.C.; Horsley, N.; Buchholz, U.J.; Openshaw, P.J.; McLellan, J.S.; Englund, J.A.; et al. The respiratory syncytial virus vaccine landscape: Lessons from the graveyard and promising candidates. *Lancet Infect. Dis.* **2018**, *18*, e295–e311. [[CrossRef](#)]
9. Collins, P.L.; Fearn, R.; Graham, B.S. Respiratory Syncytial Virus: Virology, Reverse Genetics, and Pathogenesis of Disease. In *Challenges and Opportunities for Respiratory Syncytial Virus Vaccines. Current Topics in Microbiology and Immunology*; Anderson, L.J., Graham, B.S., Eds.; Springer: Berlin/Heidelberg, Germany, 2013; Volume 372, pp. 3–38.
10. Anderson, L.J. Respiratory syncytial virus vaccine development. *Semin. Immunol.* **2013**, *25*, 160–171. [[CrossRef](#)]
11. Schepens, B.; Sedeyn, K.; Vande Ginste, L.; De Baets, S.; Schotsaert, M.; Roose, K.; Houspie, L.; Van Ranst, M.; Gilbert, B.; van Rooijen, N.; et al. Protection and mechanism of action of a novel human respiratory syncytial virus vaccine candidate based on the extracellular domain of small hydrophobic protein. *EMBO Mol. Med.* **2014**, *6*, 1436–1454. [[CrossRef](#)]
12. Ngwuta, J.O.; Chen, M.; Modjarrad, K.; Joyce, M.G.; Kanekiyo, M.; Kumar, A.; Yassine, H.M.; Moin, S.M.; Killikelly, A.M.; Chuang, G.Y.; et al. Prefusion F-specific antibodies determine the magnitude of RSV neutralizing activity in human sera. *Sci. Transl. Med.* **2015**, *7*, 309ra162. [[CrossRef](#)] [[PubMed](#)]
13. Graham, B.S. Immunological goals for respiratory syncytial virus vaccine development. *Curr. Opin. Immunol.* **2019**, *59*, 57–64. [[CrossRef](#)] [[PubMed](#)]
14. Tripp, R.A.; Power, U.F.; Openshaw, P.J.M.; Kauvar, L.M. Respiratory Syncytial Virus: Targeting the G Protein Provides a New Approach for an Old Problem. *J. Virol.* **2018**, *92*. [[CrossRef](#)] [[PubMed](#)]
15. Tripp, R.A. CX3C chemokine mimicry by respiratory syncytial virus G glycoprotein. In *Chemokines in Viral Infection*; Mahalingam, S., Ed.; Landes Bioscience: Austin, TX, USA, 2003.
16. Boyoglu-Barnum, S.; Gaston, K.A.; Todd, S.O.; Boyoglu, C.; Chirkova, T.; Barnum, T.R.; Jorquera, P.; Haynes, L.M.; Tripp, R.A.; Moore, M.L.; et al. A respiratory syncytial virus (RSV) anti-G protein F(ab')₂ monoclonal antibody suppresses mucous production and breathing effort in RSV rA2-line19F-infected BALB/c mice. *J. Virol.* **2013**, *87*, 10955–10967. [[CrossRef](#)]
17. Boyoglu-Barnum, S.; Todd, S.O.; Chirkova, T.; Barnum, T.R.; Gaston, K.A.; Haynes, L.M.; Tripp, R.A.; Moore, M.L.; Anderson, L.J. An anti-G protein monoclonal antibody treats RSV disease more effectively than an anti-F monoclonal antibody in BALB/c mice. *Virology* **2015**, *483*, 117–125. [[CrossRef](#)]
18. Radu, G.U.; Caidi, H.; Miao, C.; Tripp, R.A.; Anderson, L.J.; Haynes, L.M. Prophylactic treatment with a G glycoprotein monoclonal antibody reduces pulmonary inflammation in respiratory syncytial virus (RSV)-challenged naive and formalin-inactivated RSV-immunized BALB/c mice. *J. Virol.* **2010**, *84*, 9632–9636. [[CrossRef](#)]

19. Rey, G.U.; Miao, C.; Caidi, H.; Trivedi, S.U.; Harcourt, J.L.; Tripp, R.A.; Anderson, L.J.; Haynes, L.M. Decrease in formalin-inactivated respiratory syncytial virus (FI-RSV) enhanced disease with RSV G glycoprotein peptide immunization in BALB/c mice. *PLoS ONE* **2013**, *8*, e83075. [[CrossRef](#)]
20. Jorquera, P.A.; Choi, Y.; Oakley, K.E.; Powell, T.J.; Boyd, J.G.; Palath, N.; Haynes, L.M.; Anderson, L.J.; Tripp, R.A. Nanoparticle vaccines encompassing the respiratory syncytial virus (RSV) G protein CX3C chemokine motif induce robust immunity protecting from challenge and disease. *PLoS ONE* **2013**, *8*, e74905. [[CrossRef](#)]
21. Zhang, W.; Choi, Y.; Haynes, L.M.; Harcourt, J.L.; Anderson, L.J.; Jones, L.P.; Tripp, R.A. Vaccination to induce antibodies blocking the CX3C-CX3CR1 interaction of respiratory syncytial virus G protein reduces pulmonary inflammation and virus replication in mice. *J. Virol.* **2010**, *84*, 1148–1157. [[CrossRef](#)]
22. Chirkova, T.; Lin, S.; Oomens, A.G.; Gaston, K.A.; Boyoglu-Barnum, S.; Meng, J.; Stobart, C.C.; Cotton, C.U.; Hartert, T.V.; Moore, M.L.; et al. CX3CR1 is an important surface molecule for respiratory syncytial virus infection in human airway epithelial cells. *J. Gen. Virol.* **2015**, *96*, 2543–2556. [[CrossRef](#)]
23. Johnson, S.M.; McNally, B.A.; Ioannidis, I.; Flano, E.; Teng, M.N.; Oomens, A.G.; Walsh, E.E.; Peeples, M.E. Respiratory Syncytial Virus Uses CX3CR1 as a Receptor on Primary Human Airway Epithelial Cultures. *PLoS Pathog.* **2015**, *11*, e1005318. [[CrossRef](#)] [[PubMed](#)]
24. Stokes, K.L.; Currier, M.G.; Sakamoto, K.; Lee, S.; Collins, P.L.; Plemper, R.K.; Moore, M.L. The respiratory syncytial virus fusion protein and neutrophils mediate the airway mucin response to pathogenic respiratory syncytial virus infection. *J. Virol.* **2013**, *87*, 10070–10082. [[CrossRef](#)]
25. Meng, J.; Hotard, A.L.; Currier, M.G.; Lee, S.; Stobart, C.C.; Moore, M.L. Respiratory Syncytial Virus Attachment Glycoprotein Contribution to Infection Depends on the Specific Fusion Protein. *J. Virol.* **2015**, *90*, 245–253. [[CrossRef](#)] [[PubMed](#)]
26. Kiss, G.; Holl, J.M.; Williams, G.M.; Alonas, E.; Vanover, D.; Lifland, A.W.; Gudheti, M.; Guerrero-Ferreira, R.C.; Nair, V.; Yi, H.; et al. Structural analysis of respiratory syncytial virus reveals the position of M2-1 between the matrix protein and the ribonucleoprotein complex. *J. Virol.* **2014**, *88*, 7602–7617. [[CrossRef](#)] [[PubMed](#)]
27. Yi, H.; Strauss, J.D.; Ke, Z.; Alonas, E.; Dillard, R.S.; Hampton, C.M.; Lamb, K.M.; Hammonds, J.E.; Santangelo, P.J.; Spearman, P.W.; et al. Native immunogold labeling of cell surface proteins and viral glycoproteins for cryo-electron microscopy and cryo-electron tomography applications. *J. Histochem. Cytochem.* **2015**, *63*, 780–792. [[CrossRef](#)] [[PubMed](#)]
28. Murawski, M.R.; McGinnes, L.W.; Finberg, R.W.; Kurt-Jones, E.A.; Massare, M.J.; Smith, G.; Heaton, P.M.; Fraire, A.E.; Morrison, T.G. Newcastle disease virus-like particles containing respiratory syncytial virus G protein induced protection in BALB/c mice, with no evidence of immunopathology. *J. Virol.* **2010**, *84*, 1110–1123. [[CrossRef](#)]
29. Quan, F.S.; Kim, Y.; Lee, S.; Yi, H.; Kang, S.M.; Bozja, J.; Moore, M.L.; Compans, R.W. Viruslike particle vaccine induces protection against respiratory syncytial virus infection in mice. *J. Infect. Dis.* **2011**, *204*, 987–995. [[CrossRef](#)] [[PubMed](#)]
30. Schwarz, B.; Morabito, K.M.; Ruckwardt, T.J.; Patterson, D.P.; Avera, J.; Miettinen, H.M.; Graham, B.S.; Douglas, T. Viruslike Particles Encapsidating Respiratory Syncytial Virus M and M2 Proteins Induce Robust T Cell Responses. *ACS Biomater. Sci. Eng.* **2016**, *2*, 2324–2332. [[CrossRef](#)]
31. Meshram, C.D.; Baviskar, P.S.; Ognibene, C.M.; Oomens, A.G.P. The Respiratory Syncytial Virus Phosphoprotein, Matrix Protein, and Fusion Protein Carboxy-Terminal Domain Drive Efficient Filamentous Virus-Like Particle Formation. *J. Virol.* **2016**, *90*, 10612–10628. [[CrossRef](#)]
32. Shaikh, F.Y.; Cox, R.G.; Lifland, A.W.; Hotard, A.L.; Williams, J.V.; Moore, M.L.; Santangelo, P.J.; Crowe, J.E., Jr. A critical phenylalanine residue in the respiratory syncytial virus fusion protein cytoplasmic tail mediates assembly of internal viral proteins into viral filaments and particles. *mBio* **2012**, *3*. [[CrossRef](#)]
33. Walpita, P.; Johns, L.M.; Tandon, R.; Moore, M.L. Mammalian Cell-Derived Respiratory Syncytial Virus-Like Particles Protect the Lower as well as the Upper Respiratory Tract. *PLoS ONE* **2015**, *10*, e0130755. [[CrossRef](#)] [[PubMed](#)]
34. Stone, A.B. A simplified method for preparing sucrose gradients. *Biochem. J.* **1974**, *137*, 117–118. [[CrossRef](#)]
35. Ramakrishnan, M.A. Determination of 50% endpoint titer using a simple formula. *World J. Virol.* **2016**, *5*, 85–86. [[CrossRef](#)]
36. Booth, D.S.; Avila-Sakar, A.; Cheng, Y. Visualizing proteins and macromolecular complexes by negative stain EM: From grid preparation to image acquisition. *J. Vis. Exp.* **2011**. [[CrossRef](#)] [[PubMed](#)]

37. Jung, M.K.; Mun, J.Y. Sample Preparation and Imaging of Exosomes by Transmission Electron Microscopy. *J. Vis. Exp.* **2018**. [[CrossRef](#)] [[PubMed](#)]
38. Zhang, L.; Tong, H.; Garewal, M.; Ren, G. Optimized negative-staining electron microscopy for lipoprotein studies. *Biochim. Biophys. Acta* **2013**, *1830*, 2150–2159. [[CrossRef](#)]
39. Kremer, J.R.; Mastronarde, D.N.; McIntosh, J.R. Computer visualization of three-dimensional image data using IMOD. *J. Struct. Biol.* **1996**, *116*, 71–76. [[CrossRef](#)]
40. Olson, E. Particle shape factors and their use in image analysis—Part 1: Theory. *J. GXP Compliance* **2011**, *15*, 85–96.
41. Moore, M.L.; Chi, M.H.; Luongo, C.; Lukacs, N.W.; Polosukhin, V.V.; Huckabee, M.M.; Newcomb, D.C.; Buchholz, U.J.; Crowe, J.E., Jr.; Goleniewska, K.; et al. A chimeric A2 strain of respiratory syncytial virus (RSV) with the fusion protein of RSV strain line 19 exhibits enhanced viral load, mucus, and airway dysfunction. *J. Virol.* **2009**, *83*, 4185–4194. [[CrossRef](#)]
42. Boyoglu-Barnum, S.; Todd, S.O.; Meng, J.; Barnum, T.R.; Chirkova, T.; Haynes, L.M.; Jadhao, S.J.; Tripp, R.A.; Oomens, A.G.; Moore, M.L.; et al. Mutating the CX3C Motif in the G Protein Should Make a Live Respiratory Syncytial Virus Vaccine Safer and More Effective. *J. Virol.* **2017**, *91*. [[CrossRef](#)]
43. Ke, Z.; Dillard, R.S.; Chirkova, T.; Leon, F.; Stobart, C.C.; Hampton, C.M.; Strauss, J.D.; Rajan, D.; Rostad, C.A.; Taylor, J.V.; et al. The Morphology and Assembly of Respiratory Syncytial Virus Revealed by Cryo-Electron Tomography. *Viruses* **2018**, *10*, 446. [[CrossRef](#)] [[PubMed](#)]
44. Jeong, K.I.; Piepenhagen, P.A.; Kishko, M.; DiNapoli, J.M.; Groppo, R.P.; Zhang, L.; Almond, J.; Kleantous, H.; Delagrave, S.; Parrington, M. CX3CR1 Is Expressed in Differentiated Human Ciliated Airway Cells and Co-Localizes with Respiratory Syncytial Virus on Cilia in a G Protein-Dependent Manner. *PLoS ONE* **2015**, *10*, e0130517. [[CrossRef](#)] [[PubMed](#)]
45. Li, D.; Jans, D.A.; Bardin, P.G.; Meanger, J.; Mills, J.; Ghildyal, R. Association of respiratory syncytial virus M protein with viral nucleocapsids is mediated by the M2-1 protein. *J. Virol.* **2008**, *82*, 8863–8870. [[CrossRef](#)] [[PubMed](#)]
46. Fearn, R.; Collins, P.L. Role of the M2-1 transcription antitermination protein of respiratory syncytial virus in sequential transcription. *J. Virol.* **1999**, *73*, 5852–5864. [[CrossRef](#)] [[PubMed](#)]
47. Tanner, S.J.; Ariza, A.; Richard, C.A.; Kyle, H.F.; Dods, R.L.; Blondot, M.L.; Wu, W.; Trincao, J.; Trinh, C.H.; Hiscox, J.A.; et al. Crystal structure of the essential transcription antiterminator M2-1 protein of human respiratory syncytial virus and implications of its phosphorylation. *Proc. Natl. Acad. Sci. USA* **2014**, *111*, 1580–1585. [[CrossRef](#)] [[PubMed](#)]
48. Cowton, V.M.; McGivern, D.R.; Fearn, R. Unravelling the complexities of respiratory syncytial virus RNA synthesis. *J. Gen. Virol.* **2006**, *87*, 1805–1821. [[CrossRef](#)]
49. Bakker, S.E.; Duquerroy, S.; Galloux, M.; Loney, C.; Conner, E.; Eleouet, J.F.; Rey, F.A.; Bhella, D. The respiratory syncytial virus nucleoprotein-RNA complex forms a left-handed helical nucleocapsid. *J. Gen. Virol.* **2013**, *94*, 1734–1738. [[CrossRef](#)]
50. Tawar, R.G.; Duquerroy, S.; Vonnrhein, C.; Varela, P.F.; Damier-Piolle, L.; Castagne, N.; MacLellan, K.; Bedouelle, H.; Bricogne, G.; Bhella, D.; et al. Crystal structure of a nucleocapsid-like nucleoprotein-RNA complex of respiratory syncytial virus. *Science* **2009**, *326*, 1279–1283. [[CrossRef](#)]
51. Esperante, S.A.; Paris, G.; de Prat-Gay, G. Modular unfolding and dissociation of the human respiratory syncytial virus phosphoprotein p and its interaction with the m(2-1) antiterminator: A singular tetramer-tetramer interface arrangement. *Biochemistry* **2012**, *51*, 8100–8110. [[CrossRef](#)]
52. Connors, M.; Collins, P.L.; Firestone, C.-Y.; Murphy, B.R. Respiratory syncytial virus (RSV) F, G, M2 (22K), and N proteins each induce resistance to RSV Challenge, but resistance induced by M2 and N proteins is relatively short-lived. *J. Virol.* **1991**, *65*, 1634–1637. [[CrossRef](#)]
53. Green, C.A.; Scarselli, E.; Sande, C.J.; Thompson, A.J.; de Lara, C.M.; Taylor, K.S.; Haworth, K.; Del Sorbo, M.; Angus, B.; Siani, L.; et al. Chimpanzee adenovirus- and MVA-vectored respiratory syncytial virus vaccine is safe and immunogenic in adults. *Sci. Transl. Med.* **2015**, *7*, 300ra126. [[CrossRef](#)] [[PubMed](#)]
54. McLellan, J.S.; Ray, W.C.; Peeples, M.E. Structure and function of respiratory syncytial virus surface glycoproteins. *Curr. Top. Microbiol. Immunol.* **2013**, *372*, 83–104. [[CrossRef](#)] [[PubMed](#)]

55. McLellan, J.S.; Chen, M.; Joyce, M.G.; Sastry, M.; Stewart-Jones, G.B.; Yang, Y.; Zhang, B.; Chen, L.; Srivatsan, S.; Zheng, A.; et al. Structure-based design of a fusion glycoprotein vaccine for respiratory syncytial virus. *Science* **2013**, *342*, 592–598. [[CrossRef](#)] [[PubMed](#)]
56. Krarup, A.; Truan, D.; Furmanova-Hollenstein, P.; Bogaert, L.; Bouchier, P.; Bisschop, I.J.M.; Widjoatmodjo, M.N.; Zahn, R.; Schuitemaker, H.; McLellan, J.S.; et al. A highly stable prefusion RSV F vaccine derived from structural analysis of the fusion mechanism. *Nat. Commun.* **2015**, *6*, 8143. [[CrossRef](#)] [[PubMed](#)]



© 2020 by the authors. Licensee MDPI, Basel, Switzerland. This article is an open access article distributed under the terms and conditions of the Creative Commons Attribution (CC BY) license (<http://creativecommons.org/licenses/by/4.0/>).